Graphitized nanocarbon-supported metal catalysts: synthesis, properties, and applications in heterogeneous catalysis

Fei Huang[1,2], Hongyang Liu[1*] and Dangsheng Su[1]

ABSTRACT Graphitized nanocarbon materials can be an ideal catalyst support for heterogeneous catalytic systems. Their unique physical and chemical properties, such as large surface area, high adsorption capacity, excellent thermal and mechanical stability, outstanding electronic properties, and tunable porosity, allow the anchoring and dispersion of the active metals. Therefore, currently they are used as the key support material in many catalytic processes. This review summarizes recent relevant applications in supported catalysts that use graphitized nanocarbon as supports for catalytic oxidation, hydrogenation, dehydrogenation, and C–C coupling reactions in liquid-phase and gas-solid phase-reaction systems. The latest developments in specific features derived from the morphology and characteristics of graphitized nanocarbon-supported metal catalysts are highlighted, as well as the differences in the catalytic behavior of graphitized nanocarbon-supported metal catalysts *versus* other related catalysts. The scientific challenges and opportunities in this field are also discussed.

Keywords: nanocarbon materials; graphitized carbon supports; metal catalysts; hetergeneous catalysis

INTRODUCTION

Carbon combines its atoms in diverse hybridization states (sp, sp^2, sp^3) to form a variety of polymorphs. These are composed entirely of carbon but have different physical structures and different names, including diamond, graphite, fullerenes, and carbines, among others [1–5]. Because these various and versatile allotropes produce materials with a large range of properties, carbon materials can be used in a number of technological processes, including high-tech catalytic ones [6–10].

In heterogeneous catalysis, carbon material plays well-established and important roles in a wide range of applications, both as catalyst in its own right and as a unique support material [11–15]. The chemical stability of carbon supports in some specifically aqueous phase biomass conversion surpasses that of metal oxide materials; in addition, carbon materials present other common and key advantages as support materials for catalysis [1,5]. From the point of physical structure, porous carbon can be prepared in different forms (granules, cloth, fibers, pallets, etc.). Due to its chemical properties, carbon structure is resistant to both acidic and basic media. The structure of carbon is stable at high temperature (even above 1023 K under inert atmosphere). The hydrophilic/hydrophobic nature of carbon can be easily modified. Active metals on the support can be easily reduced. For the purposes of industrial economy and environment, the active phase can be easily recovered. Conventional carbon supports are lower-cost and more easily available than other conventional supports.

Although several kinds of carbon materials have been studied, active carbon (AC) [12,16–19] and, to a lesser extend, carbon black [20–23] have long been the most commonly used carbon supports. AC is an amorphous solid prepared by physical or chemical activation. Carbon black is an amorphous carbon derived from the pyrolysis of organic polymers or hydrocarbon precursors. As the materials of choice for most commonly used carbon supports, their feature benefits include high surface areas, low costs, and mass availability. However, their electrical conductivity is barely satisfactory [1,12,24–26]. AC also suffers from its microporous structure, which restricts the mass transfer of gas molecules in gas-solid phase catalytic reactions and leads to gathering and carbonizing small organic molecules at high reaction temperature. In ad-

[1] Shenyang National Laboratory for Materials Science, Institute of Metal Research, Chinese Academy of Sciences, Shenyang 110016, China
[2] School of Materials Science and Engineering, University of Science and Technology of China, Hefei 230026, China
* Corresponding author (email: liuhy@imr.ac.cn)

dition, carbon deposition on a catalyst surface leads to the active site covered and the deactivation of the catalyst. Since the first experimental isolation of graphene in 2004, the synthesis and applications of carbon materials have become a hot topic in catalysis [27–36]. Compared to other carbon allotropes, graphene offers the greatest intrinsic carrier mobility at room temperature; its perfect atom lattice promises mechanical strength, chemical and thermal stability, high adsorption capacity, excellent electrical conductivity, and easiness of modification, making it an ideal choice for catalyst support [37–41].

It is worth noting that, due to the nature of two dimensional (2D) material, graphene tends to form irreversible agglomerates *via* van der Waals interactions [42–44]. The key challenges involve preventing the stacking of graphene sheets and achieving complete dispersion of individual single-layer graphene in various solvents to support active phase. Unlike the simple agglomeration feature of 2D-structure graphene, some other 0D and/or 3D sp^2 carbon materials, such as onionlike carbon (OLC) and few-layer graphene (FLG), can be prepared easily and have been utilized and researched in catalysis as carbon supports [45–50].

All of these carbon supports can be regarded as graphitized nanocarbons because they consist primarily of sp^2 carbon atoms arranged in a hexagonal network. Therefore, in this review we call graphene and these sp^2 carbon materials graphitized nanocarbons. We also present a brief summary of these differently structured graphitized nanocarbons as carbon supports. Certainly, similar to carbon nanotubes (CNTs), carbon nanofibers (CNFs), fullerene, etc., these materials consist mainly of sp^2 carbon. As cabonaceous materials, they have been studied and applied for many years, formed their own unique systems, and been discussed in previous reviews [1,5,12,24]. The graphitized nanocarbon materials discussed herein do not include them.

Because researches about graphitized nanocarbons as catalyst supports have made considerable progress in the past few years, but reviews of their applications as supports in heterogeneous catalysis are relatively rare, it is necessary to review their applications in heterogeneous catalysis. Since several review papers have been published that cover their preparation and characterization, as well as their applications in optoelectronic chemistry [51–57], the present review does not cover electro- and photocatalysis using graphitized nanocarbon in combination with active metals. Instead, it considers catalytic reactions, from model reactions to industrially relevant reactions, and from non-selective reactions to selective

oxidation or hydrogenation reactions, dehydrogenation, and C–C coupling. Some typical preparation details, characterization results, and catalytic performance are presented, with an emphasis on the latest developments in the structure and applications of graphitized nanocarbon-supported metal catalysts.

PREPARATION OF GRAPHITIZED NANOCARBON-SUPPORTED CATALYSTS

Heterogeneous catalysts are complex assemblies, and some challenges remain in the preparation of solid-support catalysts. Minor variations in preparation conditions can significantly influence the delicate balance of conflicting demands: high activity, high selectivity, and long-term stability. Several classic synthesis methods have been developed for preparing graphitized nanocarbon-supported catalysts, including impregnation [58–62], chemical vapor deposition [63–65], precipitation and coprecipitation [47,48,66], and liquid-phase reduction [67,68]. Owing to the high surface area and excellent physical and chemical properties of graphitized nanocarbon, highly and uniformly dispersed active metals can be achieved by traditional loading methods. Of course, many reports have described novel methods to prepare graphitized nanocarbon-supported metal nanoparticles (NPs), such as the microwave-assisted method, the photochemical method, reverse micro-emulsion, and the atomic layer deposition (ALD) method.

Microwave-assisted method

Microwave heating technology needs an alternative heat source for rapid heating with shorter reaction time as well as higher reaction rate and heating homogeneity than conventional heating methods [69,70]. Microwave irradiation has been applied in the microwave-assisted synthesis of inorganic nanostructured materials, including metals [71–73], semimetals [74,75], alloys [73,76], metal oxides [77–80], metal sulfides [55,81–83], and others [84,85].

Sun and co-workers [72] reported a microwave-assisted, one-pot preparation of Pd/graphene composites with tannic acid (TA) as a reducing agent. The loading amount and size of Pd NPs could be controlled by adjusting the ration of raw materials and microwave irradiation time. Berry *et al.* [86] prepared a nanocomposite of naked Au NPs on graphene oxide (GO) sheets by microwave exposure (1.05 kW) of metal salt (HAuCl₄·3H₂O) and GO in an aqueous solution for a time interval between 60 s and 300 s with intermittent cooling after 10 s. Similar to gold (Au), different silver (Ag) nanos-
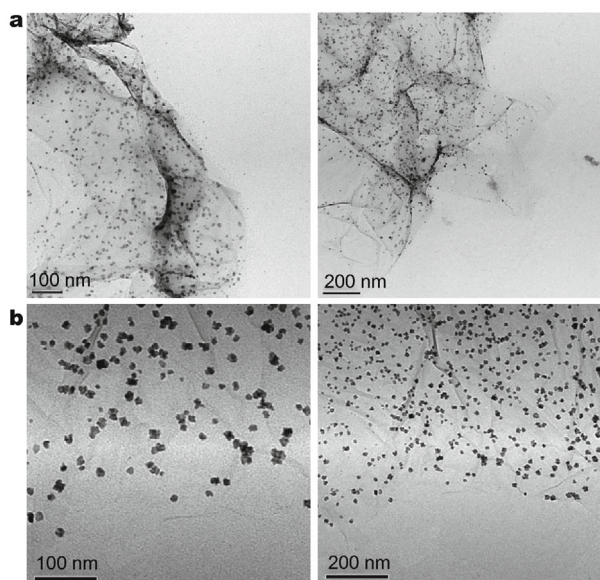
tructures (spherical and tadpole-shape) were also stabilized on GO *via* the microwave irradiation of silver salt (AgNO$_3$) in the presence of GO.

Gupton *et al.* [71] have developed a method to generate highly active Pd NPs supported on graphene (Pd/G) by microwave-assisted reduction of palladium salt (Pd(NO$_3$)$_2$). Due to the highly dispersed Pd NPs supported on graphene sheets with the small particle size of 7–9 nm (Fig. 1), Pd/G catalysts exhibited remarkable catalytic performance in Suzuki cross-coupling reaction comparable to commercial Pd/C catalyst.

Ravishankar *et al.* [87] demonstrated an ultrafast method for the formation of graphene-supported Pt catalysts by the co-reduction of GO and Pt salt using ethylene glycol under microwave irradiation conditions. The resulting hybrid consists of ultrafine NPs of Pt uniformly dispersed on the reduced GO (rGO) substrate and the hybrid exhibits good catalytic activity for methanol oxidation and hydrogen conversion reaction.

Photochemical method

The photochemical route has been developed to synthesize noble metal NPs, especially gold, silver and palladium (Pd) [88–94]. Zhang and co-workers [88–92] have done many studies on the synthesis of anisotropic Au NPs with UV irradiation of aqueous solution containing HAuCl$_4$ and template (TiO$_2$ or graphene derivatives). For this method, a graphene material with semiconducting and photocatalytic activities is required, which is combined with light and a sacrificial reducing agent [95].

Zhang *et al.* [88] developed a facile method to directly synthesize red-emission Au nanodots (NDs) (typical size <2 nm) by the photochemical reduction of HAuCl$_4$ in the presence of 1-octadecanethiol (ODT) molecules as structure director. The resulting novel *in situ*-synthesized Au NDs are self-assembled into particle chains (Fig. 2), which align along the [100] directions of the rGO lattice, directed by the thiol groups of the self-assembled ODT molecules on rGO (Fig. 3).

In other studies [90], Huang *et al.* synthesized hcp Au square sheets (AuSSs) on GO using 1-amino-9-octadecene as structure director in a solution of hexane and ethanol (Fig. 4). They also synthesized hcp/fcc square-like plates (AuSPs) through the secondary growth of hcp Au square sheets (AuSSs) on GO [91]. The AuSPs contain alternating hcp/fcc structural domains in the center and

Figure 2 Schematic illustration of the *in situ* synthesis and assembly of Au NDs on rGO. Reprinted with permission from [88]. Copyright 2010, Wiley-VCH.
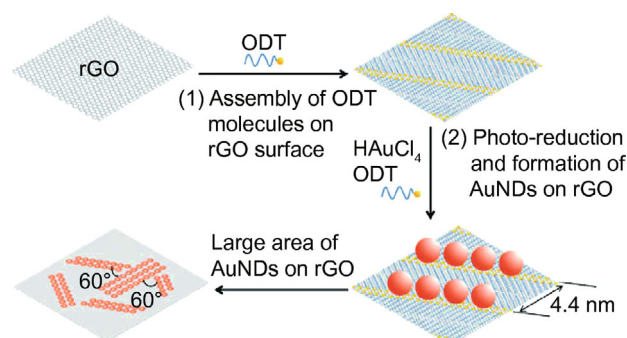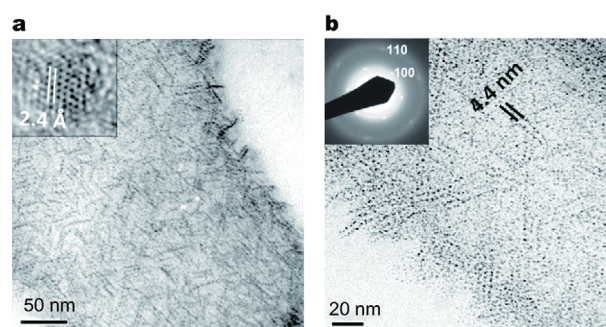

Figure 1 TEM images of (a) 7.9 wt.% Pd/G and 6.4 wt.% Pd/GO prepared by microwave irradiation of a mixture of GO and (b) palladium nitrate in the presence and absence of hydrazine hydrate. Reprinted with permission from [71]. Copyright 2010, Elsevier.

Figure 3 (a) TEM and (b) magnified TEM images of ODT-capped Au NDs synthesized *in situ* and assembled on rGO. Inset of (a) is an HRTEM image of Au NDs and inset of (b) is a selected area electron diffraction image. Reprinted with permission from [88]. Copyright 2010, Wiley-VCH.
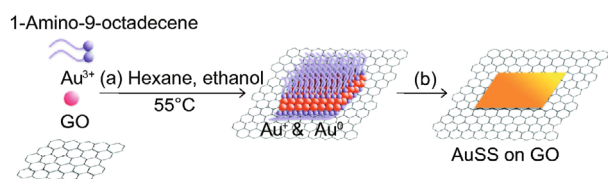
Figure 4 Schematic illustration of the *in situ* formation of hcp AuSSs on GO. Reprinted with permission from [90]. Copyright 2011, Macmillan Publishers Limited.
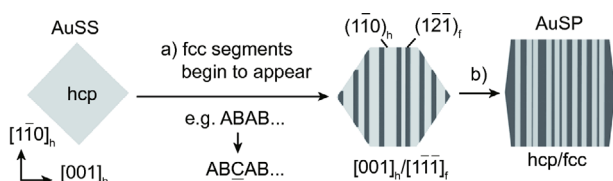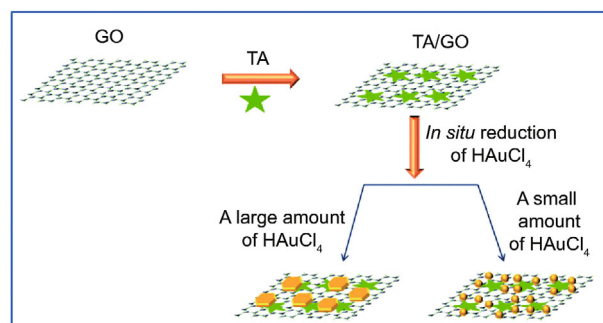

Figure 5 Schematic illustration of the shape and phase evolution of AuSS to AuSP (hcp=light gray, fcc=dark gray). Reprinted with permission from [91]. Copyright 2011, Wiley-VCH.

defect-free fcc domains at one pair of the opposite thick edges (Fig. 5).

Sun *et al.* [93] developed a green and environmentally friendly route for the synthesis of Au nanostructures on tannic acid (TA)-functionalized graphene oxide using TA as a reducing and immobilizing agent under a UV-vis spectrum (Fig. 6). Compared with *in situ* chemical reduction of gold salts using an excess amount of NaBH$_4$ as reductant, the resultant Au nanostructures/GO nanocomposites prepared by photo-induced reduction exhibit excellent catalytic activity toward 4-nitrophenol reduction.

Reverse micro-emulsions
Reverse micro-emulsions (homogenous-like combinations of water, oils, and/or surfactants) is interesting and has been confirmed as an environment-friendly alternative to the preparation of metal or metal oxide NPs [96–98]. Typically, a reverse micro-emulsion is prepared by mixing an organic solution of the surfactant with a solution of metal salt precursor to produce a solid support that is then impregnated with a micro-emulsion in a similar way to traditional chemical impregnation [99–101]. Metal NPs obtained by this method have a more controllable, narrow crystallite distribution than those obtained through traditional impregnation, co-precipitation, and precipitation–deposition methods [100–102]. Increasing the hydrophobicity of supports through a surface silylation or hydroxyl-rich treatment of supports appears to enhance the microemulsion–support
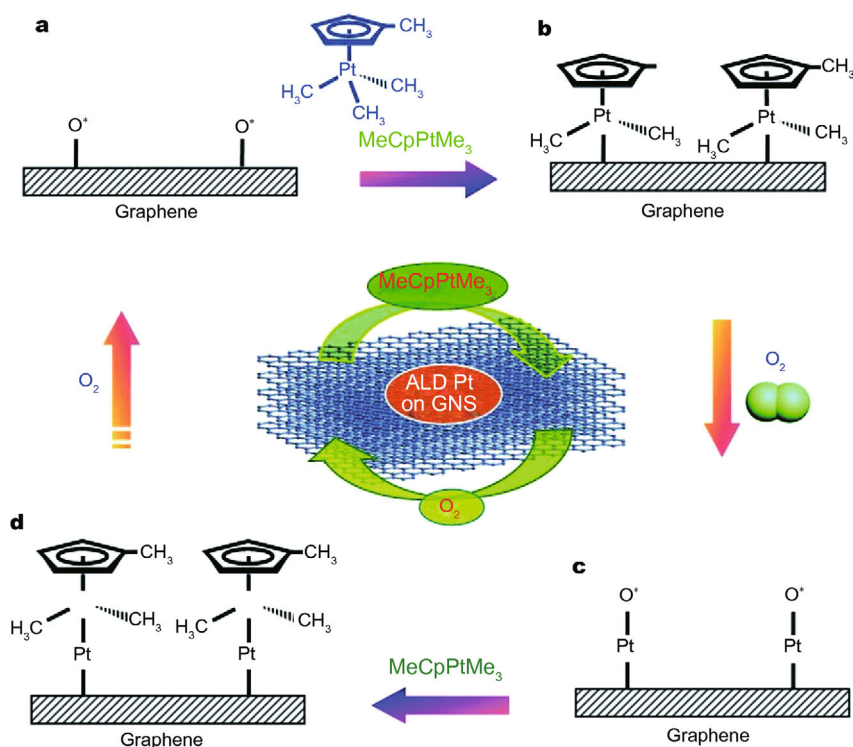

Figure 6 Schematic illustration of the noncovalent functionalization of GO by TA and the synthesis of Au/GO composites by *in situ* chemical reduction of gold salts on GO. Reprinted with permission from [93]. Copyright 2011, the Royal Society of Chemistry.

interaction and also to avoid extensive agglomeration of metal particles during deposition of metal NPs from reverse micelles [96,97]. Recently, Banerjee *et al.* [103] successfully prepared Pd/rGO composites from graphite and PdCl$_2$ precursors using a reverse micro-emulsion method. The Pd NPs were well dispersed on graphene sheets with size in the range of 6–9 nm.

Atomic layer deposition method
Atomic layer deposition (ALD) originates from a modified version of metal-organic chemical vapor deposition that relies on the self-limiting chemistry of precursors and the interaction between substrates and precursors, and is able to meet the needs of atomic level control and conformal deposition using sequential, self-limiting reaction [104–107]. ALD, which has emerged as an important technique to fabricate catalysts with atomically precise design and control, has been utilized to deposit ultra-thin metal on graphitized nanocarbon and other types of supports [108–111].

Hsieh *et al.* [105] reported an ALD approach for the fabrication of Pt nanocatalysts supported on GO sheets. The ALD process for forming the Pt atomic layer involved two self-limiting reactions and thereby induced the decoration of Pt on the edges of GO sheets in the presence of dangling bonds and oxygen functional groups. Sun and co-workers [109] employed the ALD technique to fabricate single atoms and sub-nanometer clusters of Pt on the surface of graphene sheets, using oxygen and (methylcyclopentadienyl)-trimethylplatinum (MeCpPtMe$_3$) as precursors (Fig. 7). The morphology, size, density, and loading amount of Pt on graphene sheets could be precisely controlled simply by adjusting the number of ALD cycles. Similarly, Lu and Wei *et al.*

Figure 7 Schematic illustration of Pt ALD mechanism on graphene sheets. Reprinted with permission from [109]. Copyright 2013, Macmillan Publishers Limited.

[112] successfully fabricated single-atom Pd on graphene sheets, using the ALD technique to control the type and amount of oxygen-functional groups on graphene for anchoring the Pd precursor, palladium hexa-fluoroacetylacettate (Pd(hfac)$_2$).

Although these methods are advantageous in terms of precisely controlling the growth and distribution of metal NPs on supports, some of them involved the use of excess reductant and additional surfactant, which are difficult to be removed and may pose some problems to catalysts. Nonetheless, ALD technique is able to meet the needs of atomic layer control and without excess surfactant and reductant. It should be noted, however, that ALD methods involve higher equipment requirements and precise operations.

## GRAPHITIZED NANOCARBON-SUPPORTED METAL FOR HETERGENEOUS CATALYSIS

The application of graphitized nanocarbon-supported catalysts in heterogeneous catalysis is primarily focused on oxidation, hydrogenation, dehydrogenation, and coupling reactions. In the following section, we summarize the previous typical studies according to the re-action type.

Oxidation reactions

CO oxidation is one of the most common and simple prototypical reactions for heterogeneous process, and is also of practical imporatnce for the removal of trace amounts of CO in fuel cell applications [113–116]. Recently, some studies using graphitized nanocarbon-supported metal catalysts for CO oxidation have attempted to obtain highly dispersed metal NPs on supports and to understand the interactions between NPs and graphitized nanocarbon.

Liu and co-workers [59] synthesized rGO-supported Pd catalysts *via* the conventional impregnation and hydrogen reduction method. The higher loading amount (10 wt.% Pd/rGO) and uniformly dispersed Pd NPs (average 2.6 nm) on the rGO displayed the highest catalytic activity, leading to a complete CO conversion at 119°C. The oxygen-containing groups was found to play a vital role in stabilizing Pd clusters on graphene. The oxygen species remaining on the graphene improve the adsorption of Pd atoms and reconstruct with the Pd NPs, leading to the formation of PdO$_x$ (Pd(II), Pd(IV)). In other studies, it was proven that Pd(II) sites caused CO oxidation at low
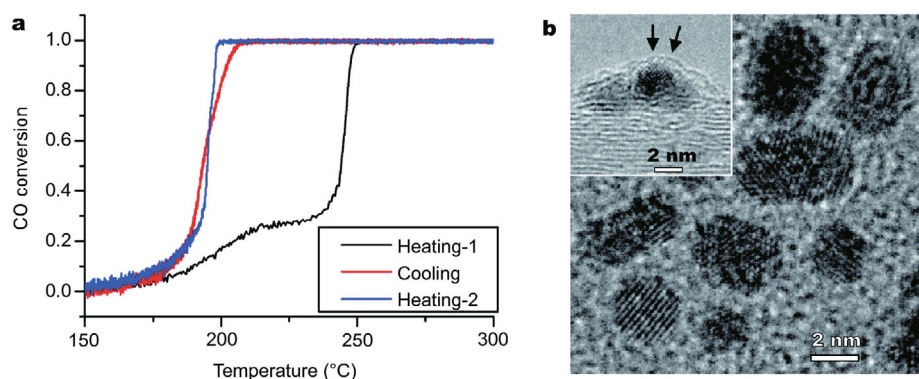
Figure 8 (a) CO oxidation depending on the reaction temperature for dispersed Pt/FLG catalyst; (b) HRTEM image of the dispersed Pt/FLG catalyst (inset shows thin amorphous carbon layer covering the platinum particle). Adapted with permission from [62]. Copyright 2015, Elsevier.
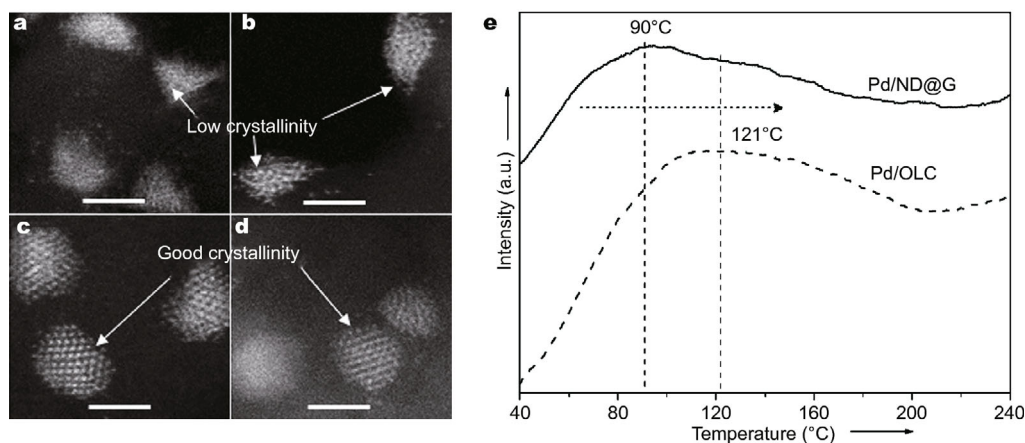

Figure 9 High-resolution HAADF-STEM images of (a, b) Pd/ND@G and (c, d) Pd/OLC (scale bar=2 nm); (e) CO-TPD spectra for Pd/ND@G and Pd/OLC. Adapted with permission from [47]. Copyright 2015, Wiley-VCH.

temperatures [117]. Stonkus and co-workers [62], who studied the activity of Pt supported on oxygen-free few-layer graphene (FLG) for CO oxidation, suggested that defects on non-oxygen-containing graphitized nano-carbon supports served as effective traps for stabilizing metal atoms or clusters. Interestingly, a thin amorphous carbon film was observed on the particle surface (Fig. 8 inset), from which they concluded that the carbon film may be partly responsible for good dispersion. Liu and Su [47] developed a novel nanodiamond-graphene material comprising a nanodiamond core and a graphitic shell with just one or two graphene layers (ND@G) by annealing nanodiamond at high temperature and used it to support Pd NPs. The Pd NPs in Pd/ND@G have irregular shapes rather than the round shape of Pd/OLC (Fig. 9a, b). In addition, from extended X-ray adsorption fine structure (EXAFS) analysis, the formation of Pd–C bonds and thus the extension of Pd–Pd bonds were observed. It

was concluded that a stronger metal-support interaction existed in Pd/ND@G and strong metal-carbon interactions with the formation of Pd–C bonds led to a charge redistribution on Pd and thus weakened the chemisorption of CO (Fig. 9e). The improvement of low-temperature CO oxidation over Pd/ND@G is the most likely result of the weakened CO chemisorption on the Pd NPs. The strong interaction between Pd and the carbon coating may also hinder Pd to form particles with well-ordered crystallinity and extended surface.

The selective oxidation of alcohols to corresponding carbonyl compounds, e.g., aldehydes or ketones, is one of the most important transformations in the synthesis of fine chemicals [61,118–121]. Traditional methods for performing such oxidation processes employ transition metal salts or organometallic complexes as homogeneous catalysts and involve inorganic oxidations, notably permanganate, chromate, bromate, and chromium(VI) re-
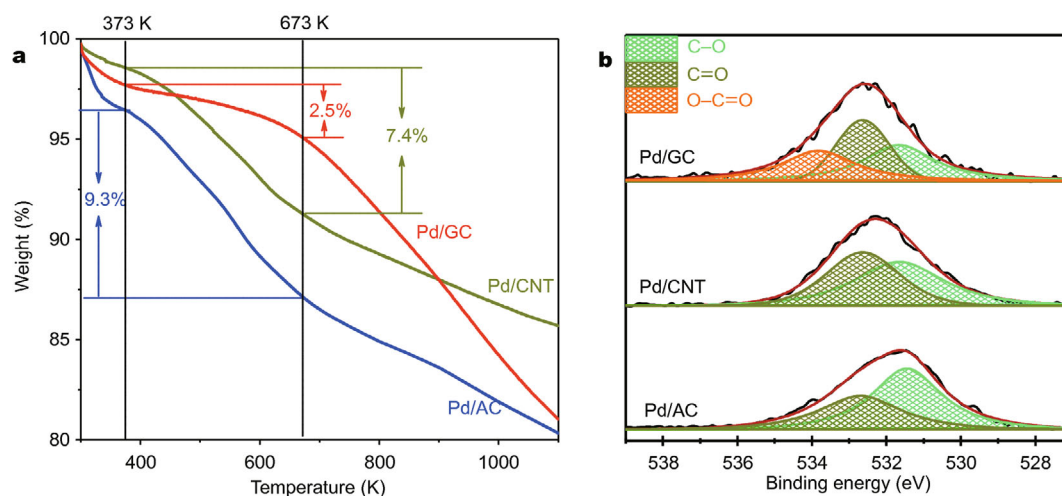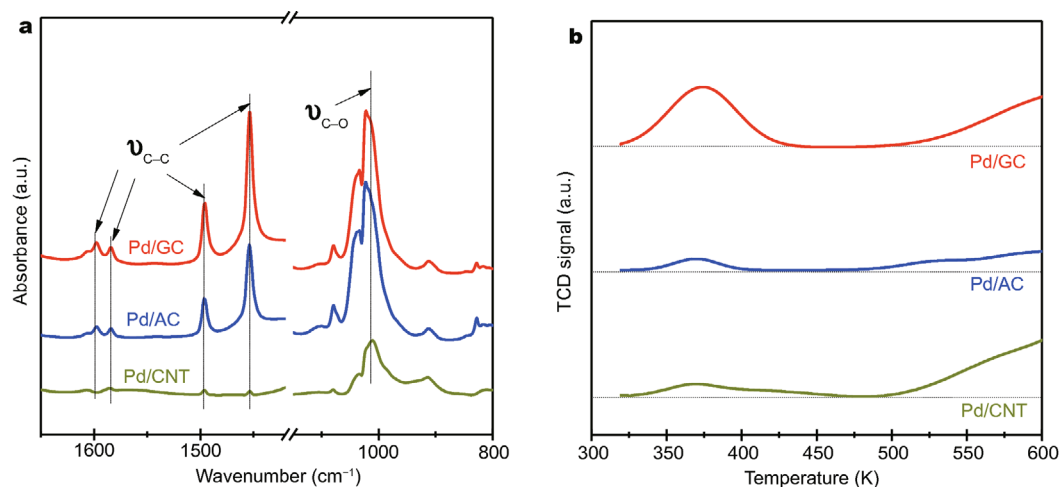
Figure 10 (a) TGA curves of Pd/GC, Pd/AC, and Pd/CNT; (b) XPS of O 1s region of Pd/GC, Pd/AC, and Pd/CNT. Adapted with permission from [61]. Copyright 2013, Elsevier.

gents. Considering environmental and economic concerns, there is a great demand for using molecular oxygen as primary oxidation [120–123]. Moreover, homogeneous catalytic systems have difficulties in catalyst separation from the reaction medium and repeated utilization. A well-designed heterogeneous catalyst may solve this dilemma because of its facile handling and reusability [122–124]. Many noble metal catalysts have been explored, e.g., Pt [125–127], Au [118,128,129], Ru [130–132], and Pd [61,123,124], as well as various supports such as Al$_2$O$_3$ [133,134], TiO$_2$ [119,120], MgO [135,136], CeO$_2$ [128,129], and SiO$_2$ [123,137], as well as carbon, for use in the liquid phase oxidation of alcohol. Specially, Pd NPs supported on carbon materials such as AC, CNTs, and hollow porous carbon spheres [138–140] are recognized as model heterogeneous catalysts for selective oxidation.

To investigate the role of graphene support for aerobic oxidation of alcohols, Li's group [61] prepared Pd catalysts supported on different carbon materials, including graphene, CNT, and AC by improved wet impregnation, and employed them in the solvent-free aerobic oxidation of aromatic alcohols using molecular oxygen as oxidant. Uniform Pd NPs with similar size (about 4 nm) were observed on different carbon supports. However, the catalytic performance was different and decreased in the sequence of Pd/G > Pd/AC > Pd/CNT. Three factors were proposed to explain the difference in activity. First, TGA results (Fig. 10a) inconsistent with the X-ray photoelectron spectroscopy (XPS) results (Fig. 10b) clearly indicate that the thermally more stable O–C=O groups only exist in Pd/GC. These surface oxygen-containing functional

groups might play an important role in stabilizing palladium species and promoting the adsorption of alcohol reactant. Second, the FTIR spectra (Fig. 11a) reveal that the adsorption of reactant benzyl alcohol is distinctively promoted on Pd/GC due to the formation of a π-electron interaction between skeleton and graphene. In addition, the O$_2$-TPD profiles (Fig. 11b) reveal that the adsorption of oxygen on Pd/GC is distinctively promoted due to oxygen spillover from palladium sites to the adjacent bridge sites of graphene. The promoted adsorption of reactant and oxygen facilitates the catalytic behavior of Pd/GC. Besides noble metal Pd, other active metals, such as Au and Ag, have also been provided for oxidation of alcohols. Das and co-workers [103] synthesized Au/rGO using ascorbic acid as a reducing agent by microwave irradiation. The spherical Au NPs on rGO were obtained with a size range of 2–20 nm and the composite performed promising catalytic activity toward the halogen- and solvent-free oxidation of substituted benzyl alcohol by O$_2$ to their corresponding aldehydes with good selectivity and yields.

Hosseini-Monfared *et al.* [58] prepared Ag NPs on thiolated-GO (GOSH) (Fig. 12) and compared Ag NPs/rGO, Ag NPs/GO, and Ag NPs/GOSH for the oxidation of benzyl alcohol by the use of molecular oxygen. Completely reduced GO is not a suitable support for Ag NPs. For stabilization of Ag NPs, the support must be functionalized, and the thiol group is a better functional group than the oxygen-containing functional group. Thiolated graphene oxide provides a uniform distribution and stabilization of Ag NPs and prevents aggregation and

Figure 11 (a) FTIR spectra of benzyl alcohol adsorption on Pd/GC, Pd/AC, and Pd/CNT; (b) O_2-TPD profiles of Pd/GC, Pd/AC, and Pd/CNT. Adapted with permission from [61]. Copyright 2013, Elsevier.
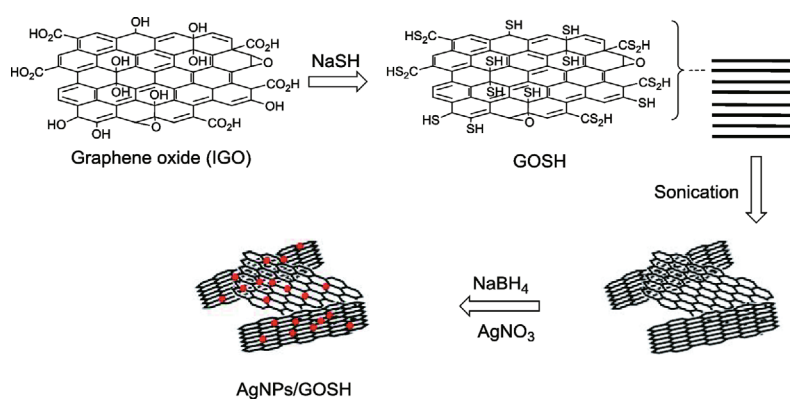
Figure 12 Schematic illustration of the synthesis of Ag NPs/GOSH by reduction of Ag^+ and GOSH. Reprinted with permission from [58]. Copyright 2014, Elsevier.

leaching of the immobilized Ag NPs. The enhanced catalytic activity of Ag NPs/GOSH is attributed to the strong adhesion between the GOSH and Ag NPs.

Hydrogenation reactions

The selective hydrogenation of multiple carbon-carbon bonds, nitroarenes, carbonyl compounds, and/or benzene rings is an important industrial process for the purification of alkene streams from petroleum cracking or to produce value-added chemicals [141–145]. Supported noble metals, particularly Pt [143,146,147], Pd [148–150], and Ru [147,151–153], are highly active catalysts for hydrogenation reactions. Recently, graphitized nanocarbon materials have also been employed as supports to catalyze this common organic transformation. Wang *et al.* [149] reported a stable Pd/G nanocomposite in the catalytic

hydrogenation of nitrophenols and nitrotolunes. The uniformly dispersed Pd NPs with a mean size of about 6.6 nm on graphene were synthesized with a hydrothermal method. The catalytic reduction of *p*-nitrophenol by adding $NaBH_4$ in an aqueous solution was chosen as a model reaction to evaluate the catalytic activities of the Pd/G and commercial Pd/C catalysts (Fig. 13). The Pd/G hybrids exhibited much higher activity and stability than the commercial Pd/C. It was found that the π–π stacking interactions may enhance adsorption of graphene, which helped promote the reaction as the reactants can easily gain access to the surface of active Pd NPs (Fig. 14). Han and co-workers [154] reported a facile one-pot synthesis of Ru/rGO *via* a solvothermal method in the presence of H_2. It was found that the small Ru NPs were uniformly embedded on the surface of the rGO sheets with a mean
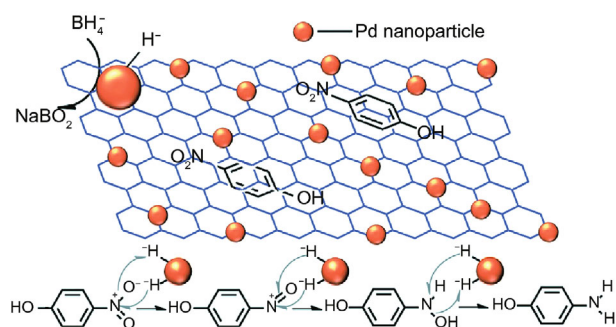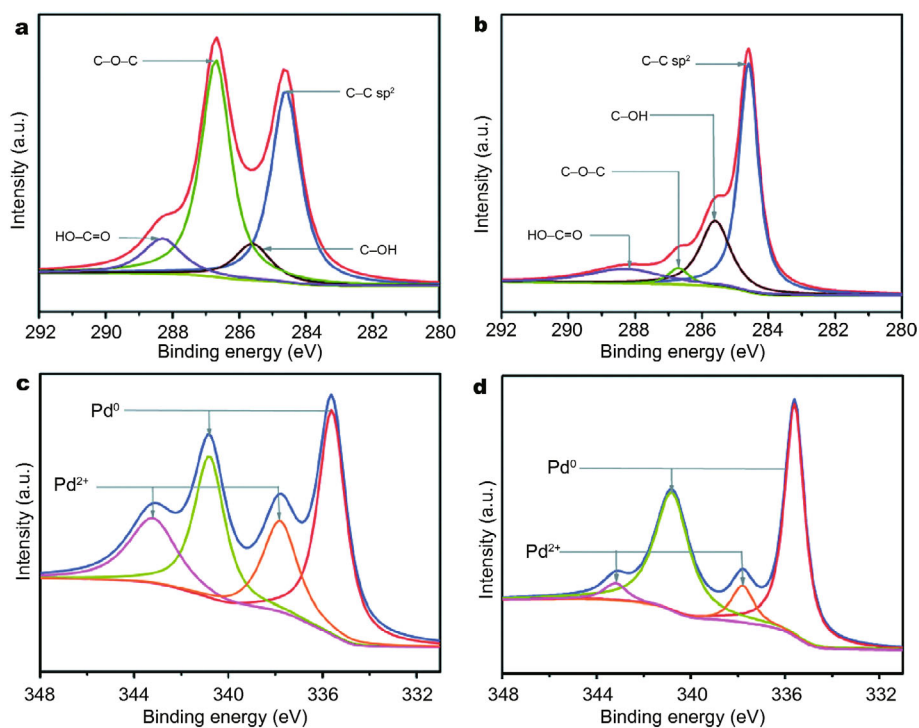
Figure 13 Schematic illustration of the mechanism for the reduction of *p*-nitrophenol catalyzed by the Pd/G catalyst in the presence of sodium borohydride. Reprinted with permission from [149]. Copyright 2014, the Royal Society of Chemistry.

ciency for hydrogenation of levulinic acid into γ-valerolactone at temperatures as low as −10°C.

Lu and Wei *et al.* [112] fabricated atomically dispersed Pd on graphene using the ALD technique. Aberration-corrected high-angle annular dark-field scanning transmission electron microscopy (HAADF-STEM) (Fig. 15d) and X-ray absorption fine structure spectroscopy (XANES) (Fig. 16a, b) both confirmed that isolated Pd single atoms were dominant on the graphene support. The single-atom Pd₁/graphene catalyst was evaluated in selective hydrogenation of 1,3-butadiene in a fixed-bed quartz tube reactor at atmospheric pressure. In selective hydrogenation of 1,3-butadiene, the single-atom Pd₁/graphene catalyst showed almost 100% butene selectivity at 95% conversion at about 50°C. The promoting catalytic behavior was mostly attributed to the changes of 1,3-butadiene adsorption mode and enhanced steric effect on the isolated Pd atoms. More importantly, excellent durability was achieved against deactivation *via* either aggregation of metal atoms or carbonaceous deposits in 100 h on stream. That study suggested that the single-atom catalysts may open up more opportunities to optimize the activity, selectivity, and durability in selective hydrogenation reactions. Truong-Huu and co-workers [60] synthesized few-layer graphenes (FLG) with a rela-

size of about 2.4 nm. The experimental data indicated that the Ru/rGO composites exhibited superior catalytic properties for the hydrogenation of halonitroaromatics to the desired amines. The conversion of halonitroaromatics reached 100% with a high selectivity of >99.6%. In addition, the Ru/rGO catalyst could be reused at least 10 times without any loss of activity. Li *et al.* [155] developed an efficient strategy for designing Ru NPs supported on rGO (Ru/rGO) catalyst. Ru/rGO shows remarkable effi-

Figure 14 XPS spectra of (a, b) the C 1s region of GO and Pd₀.₀₅/G catalyst and (c, d) the Pd 3d region of commercial Pd₀.₀₅/C and Pd₀.₀₅/GO catalyst. Reprinted with permission from [149]. Copyright 2014, the Royal Society of Chemistry.
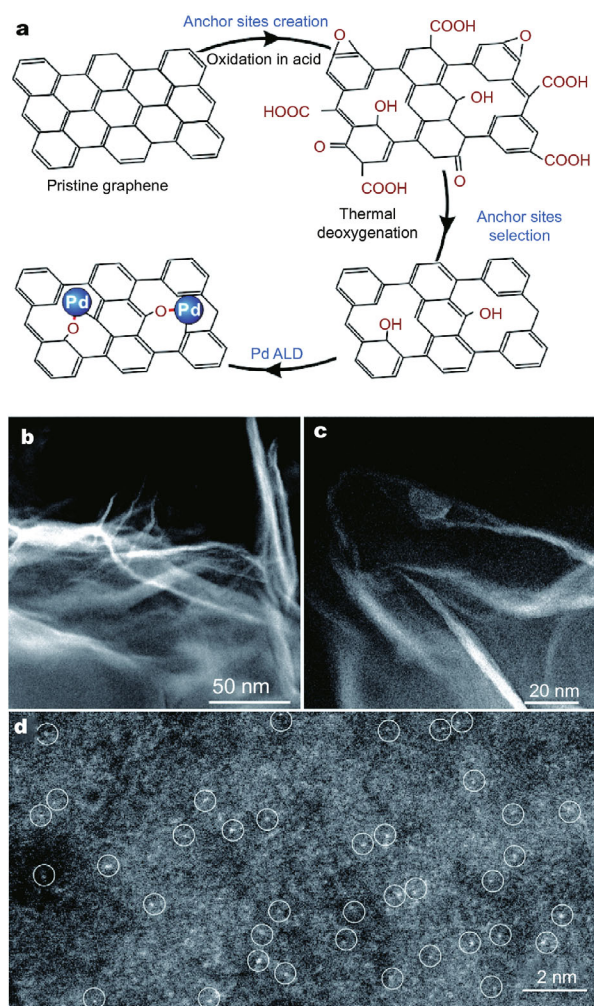
Figure 15 (a) Schematic illustration of single-atom Pd_1/graphene catalyst synthesis *via* a process of anchor sites creation and selection and Pd ALD on pristine graphene. Representative HAADF-STEM images show Pd_1/graphene at low (b, c) and high (d) magnifications. Atomically dispersed Pd atoms in image (d) are highlighted by the white circles. Reprinted with permission from [112]. Copyright 2015, the American Chemistry Society.

tively highly effective surface area through a mechanical ablation of graphite materials. Palladium NPs supported on this FLG were employed as a heterogeneous catalyst for the liquid-phase selective hydrogenation of the C=C bond. The high activity and selectivity of C=C bond hydrogenation were explained by the morphology of the support, which featured an extremely highly accessible surface for reactants and desorption of the intermediate products before secondary hydrogenation.

Dehydrogenation reactions

Dehydrogenation of hydrogen storage materials such as hydrazine monohydrate ($N_2H_4 \cdot H_2O$), ammonia borane (AB), appears to be the most favorable way to release H_2 for mobile applications and fuel cell technologies [156–161]. Önder Metin *et al.* [68] synthesized monodispersed NiPd alloy NPs (3.5 nm) by co-reduction of nickel (II) acetate and palladium (II) acetylacetonate in oleylamine (OAm) and borane-*tert*-butylamine complex (BTB) at 100°C. NiPd-alloy NPs supported on rGO (NiPd/rGO) were applied in the hydrolytic dehydrogenation of AB. The NiPd NPs show a composition-dependent catalysis with $Ni_{30}Pd_{70}$ NPs being the most active at room temperature. The NiPd/rGO performed an excellent catalytic cycle lifetime by providing a turnover number (TON) of 3,600 over 35 h. Luo and co-workers [67] prepared well-dispersed flowerlike Ni-Pt nanocluster on graphene by a simple co-reduction route, and tested hydrogen generation from alkaline solution of hydrazine. The as-synthesized Ni-Pt catalysts were also composition-dependent for catalytic activity. The as-synthesized Ni_3Pt_7/graphene composites exhibited 100% hydrogen selectivity and a remarkable turnover frequency (TOF) value of 68 h^{-1} at 25°C. The researchers attributed the promotion of catalytic activity to the unique structures and strong interaction with graphene.

The dehydrogenation of alkane is a fundamental industrial application in the chemical industry for manufacturing polymers, oxygenates, and other intermediates [162–168]. Liu *et al.* [48] prepared nanocarbon-supported (nanodiamond core and a graphitic shell) Pt NPs (Pt/ND@G). When tested for propane dehydrogenation reaction (PDH), the Pt/ND@G catalyst showed oustanding performance compared to commercial Pt/Al$_2$O$_3$. Pt NPs on ND@G exhibited superior sintering resistance *versus* the Al$_2$O$_3$ support. The temperature-programmed reduction (TPR) profiles of the Pt/ND@G and Pt/Al$_2$O$_3$ catalysts (Fig. 17a, b) showed a different reduction temperature, which was attributed to a stronger interaction between the Pt species and the support. XPS was employed to evaluate the electronic states of various supported Pt NPs. The value of Pt 4f core level for Pt/ND@G shifts to lower than that of Pt/Al$_2$O$_3$ (Fig. 17c). The differences might imply a stronger electron transference between Pt and ND@G. The superior performance of Pt/ND@G was attributed to the particular support structure of ND@G, which allows electrons on the defects to transfer to the Pt NPs, leading to a strong metal-support interaction. Similarly, Liu *et al.* [49] demonstrated the Pt/ND@G catalyst in the direct dehydrogenation (DDH) reaction of *n*-butane at a temperature as low as 450°C. An *n*-butane conversion of ~25% could be achieved at a
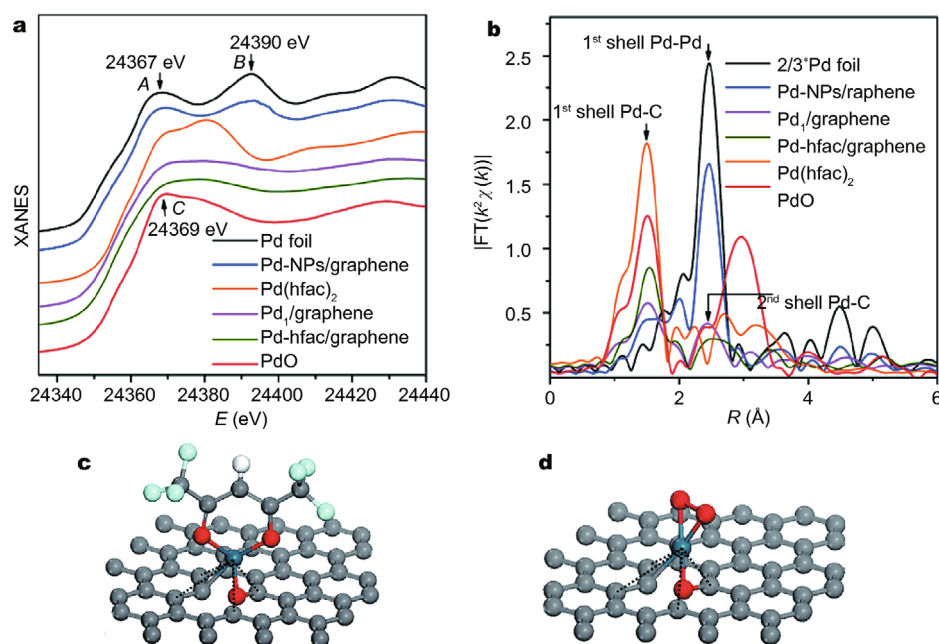
Figure 16 XANES spectra at the Pd K-edge (a) and the K_2-weighted Fourier transform spectra (b) of Pd$_1$/graphene, Pd-NPs/graphene, Pd(hfac)$_2$, PdO, and Pd foil. Schematic models of (c) Pd-hfac/graphene and (d) Pd$_1$/graphene; the gray, red, dark cyan, light blue, and white balls represent carbon, oxygen, palladium, fluorine, and hydrogen atoms, respectively. The Pd-C$_2$ coordination is indicated by the black dashed line in (c, d). Reprinted with permission from [112]. Copyright 2015, the American Chemistry Society.

temperature programmed desorption (TDP) selectivity>95%. Their *ex situ* and *in situ* TEM, in combination with XPS studies, revealed the better thermal and chemical stability of the Pt/ND@G catalysts during the reaction, given by the strong metal-support interaction (MSI) between Pt NPs and the hybrid carbon support.

C–C coupling reactions
Coupling reactions are very important transformations in synthesis of many significant organic products (pharmaceutical ingredients, optical devices, agrochemicals, natural products, materials, etc.) because of their ability to construct carbon-carbon bonds [169,170]. In 2010, Richard Heck, Ei-ichi Negishi, and Akira Suzuki jointly received the Nobel Prize for Chemistry for their roles in discovering and developing highly practical method for palladium-catalyzed cross-coupling reactions [171–173]. The typically accepted methods for coupling reactions are performed under homogeneous conditions that employ organic ligand-stabilized homogeneous complexes. Homogeneous reaction systems does contain some drawbacks, including not only the poor recovery and reusability of homogeneous catalysts but also the toxicity and water or air sensitivity [38]. Ligand-free and recyclable heterogeneous Pd catalysts represent promising op-

tions to address these issues [174,175]. The Pd NPs supported on some traditional carbon materials such as mesoporous carbon [176], AC [177], and CNTs [8] to induce coupling reactions have been developed into a distinct research area. Recently, a number of graphene-based hybrids were synthesized and employed for coupling reactions.

Zhang *et al.* [178] successfully synthesized Pd NP–graphene hybrids in a facile manner by reducing palladium acetate (Pd(OAc)$_2$) in the presence of sodium dodecyl sulfate (SDS), which was used as both surfactant and reducing agent. They demonstrated that the Pd NP–graphene hybrids can act as efficient catalysts for Suzuki reaction under aqueous and aerobic conditions, with the reaction reaching completion in 5 min. Gupton and co-workers [71] reported an efficient method to generate highly active Pd NPs supported on graphene by a microwave-assisted chemical reduction and also investigated the catalytic properties of this hybrid for C–C cross-coupling Suzuki and Heck reactions. Both Pd/G and Pd/GO demonstrated excellent catalytic activity for the carbon-carbon cross-coupling reactions under ligand-free ambient conditions in an environment-friendly solvent system. They also provided strong evidence that the outstanding reactivity and recyclability of the Pd/G cat-
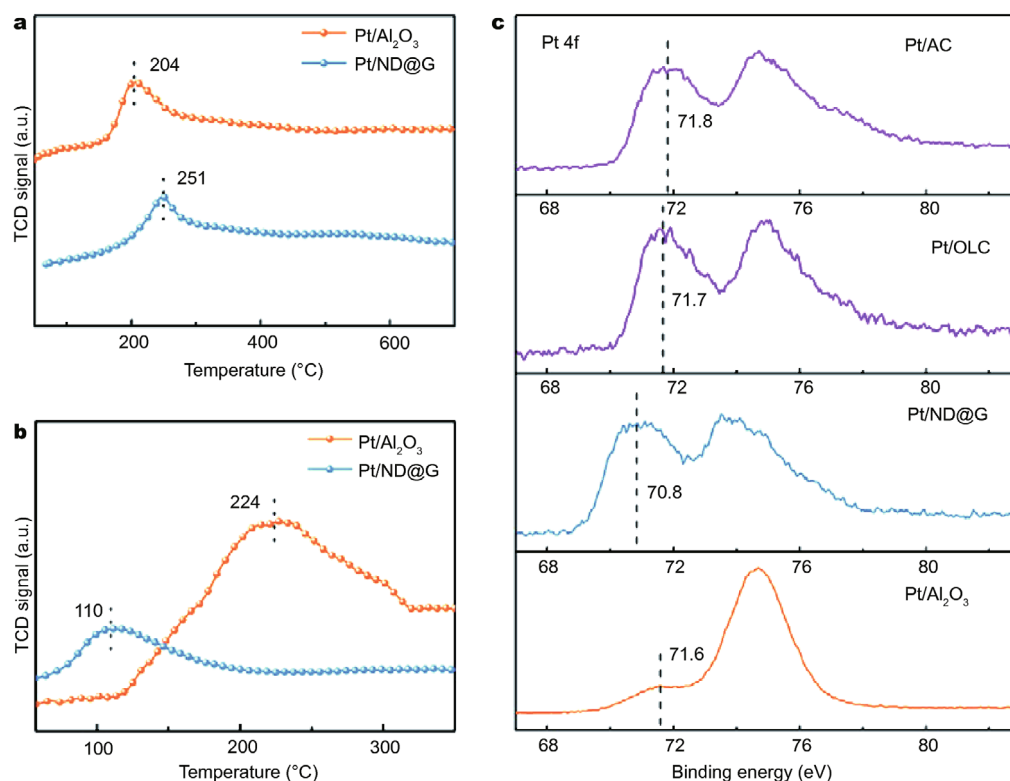
Figure 17 Characterization results for Pt/Al$_2$O$_3$, Pt/ND@G, and Pt/OLC: (a) TPR; (b) C$_3$H$_6$-TPD; and (c) XPS. The theoretical Pt weight loading of each sample was 5 wt.% for the XPS analysis; those for TPR and C$_3$H$_6$-TPD were 0.3 wt.% over Pt/Al$_2$O$_3$ and 0.5 wt.% over Pt/ND@G, respectively. Reprinted with permission from [48]. Copyright 2017, the American Chemistry Society.

alyst toward Suzuki cross-coupling reactions is associated with high concentration of Pd(0) NPs on the surface of graphene sheets. A new pulsed laser irridation method for the synthesis of Pd NPs supported on graphene was reported by El-Shall's group [179], who found Pd catalysts supported on partly rGO nanosheets (Pd/PRGO) without chemical reducing and capping agents. The redox reactions initiated by the photoexcitation of GO in different reducing environments of appropriate protic solvents (water, ethanol, and methanol) resulted in the formation of Pd NPs with different sizes supported on the PRGO sheets. The laser irradiation process led to the formation of multiple defect sites on the surface of the PRGO nanosheets, which provided an excellent environment for anchoring the Pd NPs and thereby for impeding the particles' migration and increasing the catalyst-support interaction. These results, in turn, contribute to enhanced catalytic performance as well as recyclability of the catalyst. The Pd/PRGO catalyst generated in water demonstrates excellent catalytic activity for Suzuki, Heck, and Sonogashira cross-coupling reactions, with good recyclability for Suzuki coupling with a TON of 7,800 and a

remarkable TOF of 230,000 h^{-1} at 120° C under microwave heating. Sun *et al.* [180] reported a one-pot synthesis of monodispersed 10 nm Ni/Pd core/shell NPs by sequential reduction of nickel(II) acetate and palladium (II) bromide in OAm and trioctylphosphine (TOP). The core/shell NPs were deposited on graphene sheets *via* a solution phase-based self-assembley method and were tested for utility in the Suzuki-Miyaura cross-coupling of phenyliodide and phenylboronic acid. The catalyst with the Ni/Pd molar ratio of 3/2 was the most active one, with a yield of biphenyl up to 99% when the reaction was conducted at 110°C for 10 min with DMF/H$_2$O (v/v = 7/3) as the solvent. This result is attributed to the good dispersion of the graphene support in the mixed solvent and the promotion effect of graphene in the adsorption of the aromatic reactants. Additionally, the catalyst displayed high stability, without loss in activity or noticeable leaching of metals after five cycles.

Miscellaneous reactions
Many other reaction types have been studied using metal NPs supported on graphitized nanocarbon, such as the

activation of a C–H bond in methane during the conversion of natural gas into liquid fuels [181–186], the direct synthesis of dimethylcarbonate from methanol [187–190], and the hydrochlorination of acetylene [191–193].

From the results reviewed above, we conclude that the field of graphitized nanocarbon-supported metal NPs, already a vast area of study in catalysis, has well shown that graphitized nanocarbon as a low-cost support for catalysts can be used in industry to replace current metal oxide-based catalyst supports.

CONCLUSION AND OUTLOOK

The remarkable features of graphitized nanocarbon have opened up immense possibilities for creating new kinds of carbon-based materials that represent a new class of carrier material. From this review, it is clear that graphitized nanocarbon-supported metal NPs can serve as promising catalysts for a variety of reactions and show attractive performance compared with conventional catalysts. It is noted that the defects and oxygen-containing groups on graphitized nanocarbon can provide necessary anchoring sites to stabilize the NPs. Moreover, the adsorption of reactants on the surface of catalysts driven by π–π stacking interactions can control the catalytic behavior of these catalysts.

Based on the above literature, all of which are fairly recent, the superiority and general roles of graphitized nanocarbon as a support in heterogeneous catalysis can be summarized as follows:

Graphitized nanocarbon can be derived from exfoliation of graphite carbon or deposition of hydrocarbon oxides by chemical vapor deposition. Thus the sources of graphitized nanocarbon are extensive and its synthesis and modification are controllable.

Owing to the large surface area, abundant defects and oxygen-containing groups on the surface of the graphitized nanocarbon sheets, graphitized nanocarbon is more liable to disperse and stabilize the supported metal NPs and also to retard their irreversible agglomeration and leaching from the support surface.

Stronger interaction between metal NPs and graphitized nanocarbon supports benefits hindering sintering of metal NPs and also benefits generating active phase of metal [M(II) or M(IV)] accompanied by the formation of metal-carbon bonds.

Considering the unique electronic structure of graphitized nanocarbon, the electron transfer between graphitized nanocarbon and the supported metal NPs greatly affects the catalytic selectivity.

The adsorption capacity of reactant molecules is enhanced, especially in liquid phase reaction, which originates from π–π interactions between aromatic moieties and the graphitized nanocarbon.

Due to the concept of single-atom catalysis, graphitized nanocarbon-supported single-site metal catalysts has become a hot topic and the preparation of graphitized nanocarbon-supported single-site metal catalysts faces considerable challenges. Nonetheless, both the theoretical and experimental understanding of the defects and surface functional groups has completely changed the landscape and perspectives on the use of nanocarbons as conceptually new catalyst supports. The development of characterization techniques such as microscopy and theoretical modeling, which has been both rapid and spectacular, is clearly the key to understanding the surface chemistry in detail and thereby to developing a rational design of graphitized nanocarbon for advanced catalytic applications.

1 Lam E, Luong J. Carbon materials as catalyst supports and catalysts in the transformation of biomass to fuels and chemicals. ACS Catal, 2014, 4: 3393–3410

2 Chen Y, Shi J. Mesoporous carbon biomaterials. Sci China Mater, 2015, 58: 241–257

3 Georgakilas V, Perman J, Tucek J, et al. Broad family of carbon nanoallotropes: classification, chemistry, and applications of fullerenes, carbon dots, nanotubes, graphene, nanodiamonds, and combined superstructures. Chem Rev, 2015, 115: 4744–4822

4 Falcao E, Wudl F. Carbon allotropes: beyond graphite and diamond. J Chem Technol Biotechnol, 2007, 82: 524–531

5 Serp P, Machado B. Nanostructured carbon materials for catalysis. Croydon: the Royal Society of Chemistry. 2015

6 Zhang G, Jin X, Li H, et al. N-doped crumpled graphene: bottom-up synthesis and its superior oxygen reduction performance. Sci China Mater, 2016, 59: 337–347

7 Zhang G, Xu Y, Wang L, et al. Rational design of graphene oxide and its hollow CoO composite for superior oxygen reduction reaction. Sci China Mater, 2015, 58: 534–542

8 Siamaki A, Lin Y, Woodberry K, et al. Palladium nanoparticles supported on carbon nanotubes from solventless preparations: versatile catalysts for ligand-free Suzuki cross coupling reactions. J Mater Chem A, 2013, 1: 12909–12918

9 Zheng Y, Gao M, Li H, et al. Carbon-supported $PtCo_2Ni_2$ alloy with enhanced activity and stability for oxygen reduction. Sci China Mater, 2015, 58: 179–185

10 Luo B, Huang T, Zhu Y, et al. Glucose-derived carbon sphere supported CoP as efficient and stable electrocatalysts for hydrogen evolution reaction. J Energ Chem, 2017, 26: 1147–1152

11 Su D, Perathoner S, Centi G. Nanocarbons for the development of advanced catalysts. Chem Rev, 2013, 113: 5782–5816

12 Pérez-Mayoral E, Calvino-Casilda V, Soriano E. Metal-supported carbon-based materials: opportunities and challenges in the

synthesis of valuable products. Catal Sci Technol, 2016, 6: 1265–1291

13 Xiong H, Jewell L, Coville N. Shaped carbons as supports for the catalytic conversion of syngas to clean fuels. ACS Catal, 2015, 5: 2640–2658

14 Hu C, Han Q, Zhao F, et al. Graphitic C_3N_4-Pt nanohybrids supported on a graphene network for highly efficient methanol oxidation. Sci China Mater, 2015, 58: 21–27

15 Cheng F, Li D, Lu A, et al. Controllable synthesis of high loading $LiFePO_4$/C nanocomposites using bimodal mesoporous carbon as support for high power Li-ion battery cathodes. J Energ Chem, 2013, 22: 907–913

16 Yang P, Xia Q, Liu X, et al. High-yield production of 2,5-dimethylfuran from 5-hydroxymethylfurfural over carbon supported Ni–Co bimetallic catalyst. J Energ Chem, 2016, 25: 1015–1020

17 Wang G, Xu H, Lu L, et al. Magnetization-induced double-layer capacitance enhancement in active carbon/Fe_3O_4 nanocomposites. J Energ Chem, 2014, 23: 809–815

18 Li H, Sun L, Zhang Y, et al. Enhanced cycle performance of Li/S battery with the reduced graphene oxide/activated carbon functional interlayer. J Energ Chem, 2017, 26: 1276–1281

19 Ling Y, Wang Z, Wang Z, et al. A robust carbon tolerant anode for solid oxide fuel cells. Sci China Mater, 2015, 58: 204–212

20 Luo F, Liao S, Chen D. Platinum catalysts supported on nafion functionalized carbon black for fuel cell application. J Energ Chem, 2013, 22: 87–92

21 Oschatz M, Krans N, Xie J, et al. Systematic variation of the sodium/sulfur promoter content on carbon-supported iron catalysts for the Fischer–Tropsch to olefins reaction. J Energ Chem, 2016, 25: 985–993

22 Sui S, Zhuo X, Su K, et al. In situ grown nanoscale platinum on carbon powder as catalyst layer in proton exchange membrane fuel cells (PEMFCs). J Energ Chem, 2013, 22: 477–483

23 Wu C, Yuan L, Li Z, et al. High-performance lithium-selenium battery with Se/microporous carbon composite cathode and carbonate-based electrolyte. Sci China Mater, 2015, 58: 91–97

24 Yan Y, Miao J, Yang Z, et al. Carbon nanotube catalysts: recent advances in synthesis, characterization and applications. Chem Soc Rev, 2015, 44: 3295–3346

25 Jiang W, Li Y, Han W, et al. Effect of the graphitic degree of carbon supports on the catalytic performance of ammonia synthesis over Ba-Ru-K/HSGC catalyst. J Energ Chem, 2014, 23: 443–452

26 Machado B, Marchionni A, Bacsa R, et al. Synergistic effect between few layer graphene and carbon nanotube supports for palladium catalyzing electrochemical oxidation of alcohols. J Energ Chem, 2013, 22: 296–304

27 Geim A, Novoselov K. The rise of graphene. Nat Mater, 2007, 6: 183–191

28 Tang P, Hu G, Li M, et al. Graphene-based metal-free catalysts for catalytic reactions in the liquid phase. ACS Catal, 2016, 6: 6948–6958

29 Navalon S, Dhakshinamoorthy A, Alvaro M, et al. Carbocatalysis by graphene-based materials. Chem Rev, 2014, 114: 6179–6212

30 Hu F, Patel M, Luo F, et al. Graphene-catalyzed direct Friedel–Crafts alkylation reactions: mechanism, selectivity, and synthetic utility. J Am Chem Soc, 2015, 137: 14473–14480

31 Navalon S, Dhakshinamoorthy A, Alvaro M, et al. Active sites on graphene-based materials as metal-free catalysts. Chem Soc Rev,

2017, 46: 4501–4529

32 Torres T. Graphene chemistry. Chem Soc Rev, 2017, 46: 4385–4386

33 Singh V, Joung D, Zhai L, et al. Graphene based materials: past, present and future. Prog Mater Sci, 2011, 56: 1178–1271

34 Chen D, Feng H, Li J. Graphene oxide: preparation, functionalization, and electrochemical applications. Chem Rev, 2012, 112: 6027–6053

35 Kong XK, Chen CL, Chen QW. Doped graphene for metal-free catalysis. Chem Soc Rev, 2014, 43: 2841–2857

36 Khalid M., Honorato A. Bendable tube-shaped supercapacitor based on reduced graphene oxide and Prussian blue coated carbon fiber yarns for energy storage. J Energ Chem, 2017

37 Liu M, Zhang R, Chen W. Graphene-supported nanoelectrocatalysts for fuel cells: synthesis, properties, and applications. Chem Rev, 2014, 114: 5117–5160

38 Cheng Y, Fan Y, Pei Y, et al. Graphene-supported metal/metal oxide nanohybrids: synthesis and applications in heterogeneous catalysis. Catal Sci Technol, 2015, 5: 3903–3916

39 Shang L, Bian T, Zhang B, et al. Graphene-supported ultrafine metal nanoparticles encapsulated by mesoporous silica: robust catalysts for oxidation and reduction reactions. Angew Chem, 2014, 126: 254–258

40 Han B, Liu S, Tang Z, et al. Electrostatic self-assembly of CdS nanowires-nitrogen doped graphene nanocomposites for enhanced visible light photocatalysis. J Energ Chem, 2015, 24: 145–156

41 Sun J, Zhang J, Wang L, et al. Co-salen functionalized on graphene as an efficient heterogeneous catalyst for cyclohexene oxidation. J Energ Chem, 2013, 22: 48–51

42 Dreyer D, Park S, Bielawski C, et al. The chemistry of graphene oxide. Chem Soc Rev, 2010, 39: 228–240

43 Zhu Y, Murali S, Cai W, et al. Graphene and graphene oxide: synthesis, properties, and applications. Adv Mater, 2010, 22: 3906–3924

44 Huang X, Qi X, Boey F, et al. Graphene-based composites. Chem Soc Rev, 2012, 41: 666–686

45 Xiong H, Schwartz T, Andersen N, et al. Graphitic-carbon layers on oxides: toward stable heterogeneous catalysts for biomass conversion reactions. Angew Chem Int Ed, 2015, 54: 7939–7943

46 Zang J, Wang Y, Bian L, et al. Bucky diamond produced by annealing nanodiamond as a support of Pt electrocatalyst for methanol electrooxidation. Int J Hydrogen Energ, 2012, 37: 6349–6355

47 Zhang L, Liu H, Huang X, et al. Stabilization of palladium nanoparticles on nanodiamond-graphene core-shell supports for CO oxidation. Angew Chem Int Ed, 2015, 54: 15823–15826

48 Liu J, Yue Y, Liu H, et al. Origin of the robust catalytic performance of nanodiamond–graphene-supported Pt nanoparticles used in the propane dehydrogenation reaction. ACS Catal, 2017, 7: 3349–3355

49 Liu H, Zhang J, Cai X, et al. Nanodiamond core reinforced graphene shell immobilized Pt nanoparticles as a highly active catalyst for low temperature dehydrogenation of n-butane. ChemCatChem, 2017

50 Luo W, Zafeiratos S. A brief review of the synthesis and catalytic applications of graphene-coated oxides. ChemCatChem, 2017, 9: 2432–2442

51 Li Y, Gao W, Ci L, et al. Catalytic performance of Pt nanoparticles on reduced graphene oxide for methanol electro-oxidation.

Carbon, 2010, 48: 1124–1130

52 Guo X, Hao C, Jin G, et al. Copper nanoparticles on graphene support: an efficient photocatalyst for coupling of nitroaromatics in visible light. Angew Chem Int Ed, 2014, 53: 1973–1977

53 Ding S, Luan D, Boey F, et al. SnO_2 nanosheets grown on graphene sheets with enhanced lithium storage properties. Chem Commun, 2011, 47: 7155–7157

54 Xiao YP, Wan S, Zhang X, et al. Hanging Pt hollow nanocrystal assemblies on graphene resulting in an enhanced electrocatalyst. Chem Commun, 2012, 48: 10331–10333

55 Liu X, Pan L, Lv T, et al. Microwave-assisted synthesis of CdS–reduced graphene oxide composites for photocatalytic reduction of Cr(VI). Chem Commun, 2011, 47: 11984–11986

56 An X, Yang H, Wang Y, et al. Hydrothermal synthesis of coherent porous V_2O_3/carbon nanocomposites for high-performance lithium- and sodium-ion batteries. Sci China Mater, 2017, 60: 717–727

57 Wang C, Wang J, Chen H, et al. An interlayer nanostructure of rGO/Sn_2Fe-NRs array/rGO with high capacity for lithium ion battery anodes. Sci China Mater, 2016, 59: 927–937

58 Zahed B, Hosseini-Monfared H. A comparative study of silver-graphene oxide nanocomposites as a recyclable catalyst for the aerobic oxidation of benzyl alcohol: support effect. Appl Surf Sci, 2015, 328: 536–547

59 Li Y, Yu Y, Wang J, et al. CO oxidation over graphene supported palladium catalyst. Appl Catal B-Environ, 2012, 125: 189–196

60 Truong-Huu T, Chizari K, Janowska I, et al. Few-layer graphene supporting palladium nanoparticles with a fully accessible effective surface for liquid-phase hydrogenation reaction. Catal Today, 2012, 189: 77–82

61 Wu G, Wang X, Guan N, et al. Palladium on graphene as efficient catalyst for solvent-free aerobic oxidation of aromatic alcohols: role of graphene support. Appl Catal B-Environ, 2013, 136-137: 177–185

62 Grayfer E, Kibis L, Stadnichenko A, et al. Ultradisperse Pt nanoparticles anchored on defect sites in oxygen-free few-layer graphene and their catalytic properties in CO oxidation. Carbon, 2015, 89: 290–299

63 Zhang B, Lee W, Piner R, et al. Low-temperature chemical vapor deposition growth of graphene from toluene on electropolished copper foils. ACS Nano, 2012, 6: 2471–2476

64 Guermoune A, Chari T, Popescu F, et al. Chemical vapor deposition synthesis of graphene on copper with methanol, ethanol, and propanol precursors. Carbon, 2011, 49: 4204–4210

65 Meng L, Sun Q, Wang J, et al. Molecular dynamics simulation of chemical vapor deposition graphene growth on Ni (111) surface. J Phys Chem C, 2012, 116: 6097–6102

66 Wang R, Wu Z, Chen C, et al. Graphene-supported Au–Pd bimetallic nanoparticles with excellent catalytic performance in selective oxidation of methanol to methyl formate. Chem Commun, 2013, 49: 8250–8252

67 Cao N, Yang L, Du C, et al. Highly efficient dehydrogenation of hydrazine over graphene supported flower-like Ni–Pt nanoclusters at room temperature. J Mater Chem A, 2014, 2: 14344–14347

68 Çiftci N, Metin Ö. Monodisperse nickel–palladium alloy nanoparticles supported on reduced graphene oxide as highly efficient catalysts for the hydrolytic dehydrogenation of ammonia borane. Int J Hydrogen Energ, 2014, 39: 18863–18870

69 Zhu Y, Chen F. Microwave-assisted preparation of inorganic

70 Gerbec J, Magana D, Washington A, et al. Microwave-enhanced reaction rates for nanoparticle synthesis. J Am Chem Soc, 2005, 127: 15791–15800

71 Siamaki A, Khder A, Abdelsayed V, et al. Microwave-assisted synthesis of palladium nanoparticles supported on graphene: a highly active and recyclable catalyst for carbon–carbon cross-coupling reactions. J Catal, 2011, 279: 1–11

72 Zhang Y, Chang G, Liu S, et al. Microwave-assisted, environmentally friendly, one-pot preparation of Pd nanoparticles/graphene nanocomposites and their application in electrocatalytic oxidation of methanol. Catal Sci Technol, 2011, 1: 1636–1640

73 Pal A, Shah S, Devi S. Synthesis of Au, Ag and Au–Ag alloy nanoparticles in aqueous polymer solution. Colloids Surfs A-PhysicoChem Eng Aspects, 2007, 302: 51–57

74 Zhu Y, Hu X. Preparation of powders of selenium nanorods and nanowires by microwave-polyol method. Mater Lett, 2004, 58: 1234–1236

75 Liu J, Chen F, Zhang M, et al. Rapid microwave-assisted synthesis of uniform ultralong Te nanowires, optical property, and chemical stability. Langmuir, 2010, 26: 11372–11377

76 Zhang H, Yin Y, Hu Y, et al. Pd@Pt core–shell nanostructures with controllable composition synthesized by a microwave method and their enhanced electrocatalytic activity toward oxygen reduction and methanol oxidation. J Phys Chem C, 2010, 114: 11861–11867

77 Wang W, Zhu Y, Ruan M. Microwave-assisted synthesis and magnetic property of magnetite and hematite nanoparticles. J Nanopart Res, 2007, 9: 419–426

78 Sreeja V, Joy P. Microwave–hydrothermal synthesis of γ-Fe_2O_3 nanoparticles and their magnetic properties. Mater Res Bull, 2007, 42: 1570–1576

79 Liang Z, Zhu Y. Single-crystalline CuO nanosheets synthesized from a layered precursor. Chem Lett, 2005, 34: 214–215

80 Cao C, Guo W, Cui Z, et al. Microwave-assisted gas/liquid interfacial synthesis of flowerlike NiO hollow nanosphere precursors and their application as supercapacitor electrodes. J Mater Chem, 2011, 21: 3204–3209

81 Zhao Y, Liao X, Hong J, et al. Synthesis of lead sulfide nanocrystals via microwave and sonochemical methods. Mater Chem Phys, 2004, 87: 149–153

82 Xing R, Liu S, Tian S. Microwave-assisted hydrothermal synthesis of biocompatible silver sulfide nanoworms. J Nanopart Res, 2011, 13: 4847–4854

83 Panda A, Glaspell G, El-Shall M. Microwave synthesis of highly aligned ultra narrow semiconductor rods and wires. J Am Chem Soc, 2006, 128: 2790–2791

84 Wang Z, Jia W, Jiang M, et al. Microwave-assisted synthesis of layer-by-layer ultra-large and thin NiAl-LDH/RGO nanocomposites and their excellent performance as electrodes. Sci China Mater, 2015, 58: 944–952

85 Baghbanzadeh M, Carbone L, Cozzoli P, et al. Microwave-assisted synthesis of colloidal inorganic nanocrystals. Angew Chem Int Ed, 2011, 50: 11312–11359

86 Jasuja K, Linn J, Melton S, et al. Microwave-reduced uncapped metal nanoparticles on graphene: tuning catalytic, electrical, and raman properties. J Phys Chem Lett, 2010, 1: 1853–1860

87 Kundu P, Nethravathi C, Deshpande P, et al. Ultrafast microwave-assisted route to surfactant-free ultrafine Pt nanoparticles on graphene: synergistic co-reduction mechanism and high cat-

alytic activity. Chem Mater, 2011, 23: 2772–2780

88 Huang X, Zhou X, Wu S, *et al.* Reduced graphene oxide-templated photochemical synthesis and *in situ* assembly of Au nanodots to orderly patterned Au nanodot chains. Small, 2010, 6: 513–516

89 Huang X, Qi X, Huang Y, *et al.* Photochemically controlled synthesis of anisotropic au nanostructures: platelet-like Au nanorods and six-star Au nanoparticles. ACS Nano, 2010, 4: 6196–6202

90 Huang X, Li S, Huang Y, *et al.* Synthesis of hexagonal close-packed gold nanostructures. Nat Commun, 2011, 2: 292

91 Huang X, Li H, Li S, *et al.* Synthesis of gold square-like plates from ultrathin gold square sheets: the evolution of structure phase and shape. Angew Chem Int Ed, 2011, 50: 12245–12248

92 Tan C, Huang X, Zhang H. Synthesis and applications of graphene-based noble metal nanostructures. Mater Today, 2013, 16: 29–36

93 Zhang Y, Liu S, Lu W, *et al.* In situ green synthesis of Au nanostructures on graphene oxide and their application for catalytic reduction of 4-nitrophenol. Catal Sci Technol, 2011, 1: 1142–1144

94 Liu P, Zhao Y, Qin R, *et al.* Photochemical route for synthesizing atomically dispersed palladium catalysts. Science, 2016, 352: 797–800

95 Xiang Q, Yu J, Jaroniec M. Graphene-based semiconductor photocatalysts. Chem Soc Rev, 2012, 41: 782–796

96 Martínez A, Prieto G. The key role of support surface tuning during the preparation of catalysts from reverse micellar-synthesized metal nanoparticles. Catal Commun, 2007, 8: 1479–1486

97 Campelo J , Luna D, Luque R, *et al.* Sustainable preparation of supported metal nanoparticles and their applications in catalysis. ChemSusChem, 2009, 2: 18–45

98 Sun Z, Liao T, Kou L. Strategies for designing metal oxide nanostructures. Sci China Mater, 2017, 60: 1–24

99 Cushing B, Kolesnichenko V, O'Connor C. Recent advances in the liquid-phase syntheses of inorganic nanoparticles. Chem Rev, 2004, 104: 3893–3946

100 Eriksson S. Preparation of catalysts from microemulsions and their applications in heterogeneous catalysis. Appl Catal A-General, 2004, 265: 207–219

101 Yashima M, Falk L, Palmqvist A, *et al.* Structure and catalytic properties of nanosized alumina supported platinum and palladium particles synthesized by reaction in microemulsion. J Colloid Interface Sci, 2003, 268: 348–356

102 Ruta M, Semagina N, Kiwi-Minsker L. Monodispersed Pd nanoparticles for acetylene selective hydrogenation: particle size and support effects. J Phys Chem C, 2008, 112: 13635–13641

103 Das T, Banerjee S, Pandey M, *et al.* Effect of surface functional groups on hydrogen adsorption properties of Pd dispersed reduced graphene oxide. Int J Hydrogen Energ, 2017, 42: 8032–8041

104 King J, Wittstock A, Biener J, *et al.* Ultralow loading Pt nanocatalysts prepared by atomic layer deposition on carbon aerogels. Nano Lett, 2008, 8: 2405–2409

105 Hsieh C, Chen W, Tzou D, *et al.* Atomic layer deposition of Pt nanocatalysts on graphene oxide nanosheets for electro-oxidation of formic acid. Int J Hydrogen Energ, 2012, 37: 17837–17843

106 George S. Atomic layer deposition: an overview. Chem Rev, 2010, 110: 111–131

107 O'Neill B, Jackson D, Lee J, *et al.* Catalyst design with atomic layer deposition. ACS Catal, 2015, 5: 1804–1825

108 Liu J. Catalysis by supported single metal atoms. ACS Catal, 2017, 7: 34–59

109 Sun S, Zhang G, Gauquelin N, *et al.* Single-atom catalysis using Pt/graphene achieved through atomic layer deposition. Sci Rep, 2013, 3: 1775

110 Pagán-Torres Y, Gallo J, Wang D, *et al.* Synthesis of highly ordered hydrothermally stable mesoporous niobia catalysts by atomic layer deposition. ACS Catal, 2011, 1: 1234–1245

111 Christensen S, Feng H, Libera J, *et al.* Supported Ru−Pt bimetallic nanoparticle catalysts prepared by atomic layer deposition. Nano Lett, 2010, 10: 3047–3051

112 Yan H, Cheng H, Yi H, *et al.* Single-atom Pd₁/graphene catalyst achieved by atomic layer deposition: remarkable performance in selective hydrogenation of 1,3-butadiene. J Am Chem Soc, 2015, 137: 10484–10487

113 Gao L, Fu Q, Li J, *et al.* Enhanced CO oxidation reaction over Pt nanoparticles covered with ultrathin graphitic layers. Carbon, 2016, 101: 324–330

114 Grisel R, Nieuwenhuys B. Selective oxidation of CO, over supported Au catalysts. J Catal, 2001, 199: 48–59

115 Liu J, Qiao B, Song Y, *et al.* Highly active and sintering-resistant heteroepitaxy of Au nanoparticles on ZnO nanowires for CO oxidation. J Energ Chem, 2016, 25: 361–370

116 Zhang H, Liu H. Insights into support effects on Ce-Zr–O mixed oxide-supported gold catalysts in CO oxidation. J Energ Chem, 2013, 22: 98–106

117 Schaffner I, Mlynek G, Flego N, *et al.* Atomically dispersed Pd–O species on CeO₂ (111) as highly active sites for low-temperature CO oxidation. ACS Catal, 2017, 7: 6887–6891

118 Sharma P, Darabdhara G, Reddy T, *et al.* Synthesis, characterization and catalytic application of Au NPs-reduced graphene oxide composites material: an eco-friendly approach. Catal Commun, 2013, 40: 139–144

119 Liu K, Yan X, Zou P, *et al.* Large size Pd NPs loaded on TiO₂ as efficient catalyst for the aerobic oxidation of alcohols to aldehydes. Catal Commun, 2015, 58: 132–136

120 Lu Y, Zhu H, Liu J, *et al.* Palladium nanoparticles supported on titanate nanobelts for solvent-free aerobic oxidation of alcohols. ChemCatChem, 2015, 7: 4131–4136

121 Liu K, Chen T, Hou Z, *et al.* Graphene oxide as support for the immobilization of phosphotungstic acid: application in the selective oxidation of benzyl alcohol. Catal Lett, 2014, 144: 314–319

122 Mallat T, Baiker A. Oxidation of alcohols with molecular oxygen on solid catalysts. Chem Rev, 2004, 104: 3037–3058

123 Liu K, Chen Z, Hou Z, *et al.* Sulfur-modified SBA-15 supported amorphous palladium with superior catalytic performance for aerobic oxidation of alcohols. Catal Lett, 2014, 144: 935–942

124 Mori K, Hara T, Mizugaki T, *et al.* Hydroxyapatite-supported palladium nanoclusters: a highly active heterogeneous catalyst for selective oxidation of alcohols by use of molecular oxygen. J Am Chem Soc, 2004, 126: 10657–10666

125 Bianchi C, Canton P, Dimitratos N, *et al.* Selective oxidation of glycerol with oxygen using mono and bimetallic catalysts based on Au, Pd and Pt metals. Catal Today, 2005, 102-103: 203–212

126 Li Y, Tang L, Li J. Preparation and electrochemical performance for methanol oxidation of Pt/graphene nanocomposites. ElectroChem Commun, 2009, 11: 846–849

127 Li G, Jiang L, Zhang B, *et al.* A highly active porous Pt–PbOₓ/C catalyst toward alcohol electro-oxidation in alkaline electrolyte. Int J Hydrogen Energ, 2013, 38: 12767–12773

128 Abad A, Concepción P, Corma A, *et al.* A collaborative effect between gold and a support induces the selective oxidation of alcohols. Angew Chem Int Ed, 2005, 44: 4066–4069

129 Tanaka A, Hashimoto K, Kominami H. Preparation of Au/CeO₂ exhibiting strong surface plasmon resonance effective for selective or chemoselective oxidation of alcohols to aldehydes or ketones in aqueous suspensions under irradiation by green light. J Am Chem Soc, 2012, 134: 14526–14533

130 Mondelli C, Ferri D, Baiker A. Ruthenium at work in Ru-hydroxyapatite during the aerobic oxidation of benzyl alcohol: an *in situ* ATR-IR spectroscopy study. J Catal, 2008, 258: 170–176

131 Nie J, Xie J, Liu H. Efficient aerobic oxidation of 5-hydroxymethylfurfural to 2,5-diformylfuran on supported Ru catalysts. J Catal, 2013, 301: 83–91

132 Hasheminejad E, Ojani R, Raoof J. A rapid synthesis of high surface area PdRu nanosponges: composition-dependent electrocatalytic activity for formic acid oxidation. J Energ Chem, 2017, 26: 703–711

133 Lee A, Hackett S, Hargreaves J, *et al.* On the active site in heterogeneous palladium selox catalysts. Green Chem, 2006, 8: 549–555

134 Grunwaldt J, Caravati M, Baiker A. Oxidic or metallic palladium: which is the active phase in Pd-catalyzed aerobic alcohol oxidation? J Phys Chem B, 2006, 110: 25586–25589

135 Layek K, Maheswaran H, Arundhathi R, *et al.* Nanocrystalline magnesium oxide stabilized palladium(0): an efficient reusable catalyst for room temperature selective aerobic oxidation of alcohols. Adv Synth Catal, 2011, 353: 606–616

136 Pillai U, Sahle-Demessie E. Selective oxidation of alcohols by molecular oxygen over a Pd/MgO catalyst in the absence of any additives. Green Chem, 2004, 6: 161–165

137 Parlett C, Bruce D, Hondow N, *et al.* Support-enhanced selective aerobic alcohol oxidation over Pd/mesoporous silicas. ACS Catal, 2011, 1: 636–640

138 Harada T, Ikeda S, Miyazaki M, *et al.* A simple method for preparing highly active palladium catalysts loaded on various carbon supports for liquid-phase oxidation and hydrogenation reactions. J Mol Catal A-Chem, 2007, 268: 59–64

139 Villa A, Wang D, Dimitratos N, *et al.* Pd on carbon nanotubes for liquid phase alcohol oxidation. Catal Today, 2010, 150: 8–15

140 Harada T, Ikeda S, Hashimoto F, *et al.* Catalytic activity and regeneration property of a Pd nanoparticle encapsulated in a hollow porous carbon sphere for aerobic alcohol oxidation. Langmuir, 2010, 26: 17720–17725

141 Liu H, Jiang T, Han B, *et al.* Selective phenol hydrogenation to cyclohexanone over a dual supported Pd-lewis acid catalyst. Science, 2009, 326: 1250–1252

142 Li X, Zhang W, Liu Y, *et al.* Palladium nanoparticles immobilized on magnetic porous carbon derived from ZIF-67 as efficient catalysts for the semihydrogenation of phenylacetylene under extremely mild conditions. ChemCatChem, 2016, 8: 1111–1118

143 Li C, Shao Z, Pang M, *et al.* Carbon nanotubes supported Pt catalysts for phenylacetylene hydrogenation: effects of oxygen containing surface groups on Pt dispersion and catalytic performance. Catal Today, 2012, 186: 69–75

144 Su X, Xu J, Liang B, *et al.* Catalytic carbon dioxide hydrogenation to methane: a review of recent studies. J Energ Chem, 2016, 25: 553–565

145 Huang F, Wang R, Yang C, *et al.* Catalytic performances of Ni/mesoporous SiO₂ catalysts for dry reforming of methane to hy-

drogen. J Energ Chem, 2016, 25: 709–719

146 Krooswyk J, Waluyo I, Trenary M. Simultaneous monitoring of surface and gas phase species during hydrogenation of acetylene over Pt(111) by polarization-dependent infrared spectroscopy. ACS Catal, 2015, 5: 4725–4733

147 Li C, Shao Z, Pang M, *et al.* Carbon nanotubes supported mono- and bimetallic Pt and Ru catalysts for selective hydrogenation of phenylacetylene. Ind Eng Chem Res, 2012, 51: 4934–4941

148 Pei G, Liu X, Wang A, *et al.* Ag alloyed Pd single-atom catalysts for efficient selective hydrogenation of acetylene to ethylene in excess ethylene. ACS Catal, 2015, 5: 3717–3725

149 Sun J, Fu Y, He G, *et al.* Catalytic hydrogenation of nitrophenols and nitrotoluenes over a palladium/graphene nanocomposite. Catal Sci Technol, 2014, 4: 1742–1748

150 Lee J, Kim S, Ahn I, *et al.* Performance of Pd–Ag/Al₂O₃ catalysts prepared by the selective deposition of Ag onto Pd in acetylene hydrogenation. Catal Commun, 2011, 12: 1251–1254

151 Dou Y, Pang Y, Gu L, *et al.* Core-shell structured Ru-Ni@SiO₂: active for partial oxidation of methane with tunable H₂/CO ratio. J Energy Chem

152 Wang B, Li C, He B, *et al.* Highly stable and selective Ru/NiFe₂O₄ catalysts for transfer hydrogenation of biomass-derived furfural to 2-methylfuran. J Energ Chem, 2017, 26: 799–807

153 Zhang J, Hou B, Wang X, *et al.* Inhibiting effect of tungstic compounds on glucose hydrogenation over Ru/C catalyst. J Energ Chem, 2015, 24: 9–14

154 Fan G, Huang W, Wang C. *In situ* synthesis of Ru/RGO nanocomposites as a highly efficient catalyst for selective hydrogenation of halonitroaromatics. Nanoscale, 2013, 5: 6819–6825

155 Tan J, Cui J, Cui X, *et al.* Graphene-modified Ru nanocatalyst for low-temperature hydrogenation of carbonyl groups. ACS Catal, 2015, 5: 7379–7384

156 Ren S, Huang F, Zheng J, *et al.* Ruthenium supported on nitrogen-doped ordered mesoporous carbon as highly active catalyst for NH₃ decomposition to H₂. Int J Hydrogen Energ, 2017, 42: 5105–5113

157 Suh M, Park H, Prasad T, *et al.* Hydrogen storage in metal–organic frameworks. Chem Rev, 2012, 112: 782–835

158 Luo W, Campbell P, Zakharov L, *et al.* A single-component liquid-phase hydrogen storage material. J Am Chem Soc, 2011, 133: 19326–19329

159 Tong D, Tang D, Chu W, *et al.* Monodisperse Ni₃Fe single-crystalline nanospheres as a highly efficient catalyst for the complete conversion of hydrous hydrazine to hydrogen at room temperature. J Mater Chem A, 2013, 1: 6425–6432

160 Zhang Y, Huang R, Feng Z, *et al.* Phosphate modified carbon nanotubes for oxidative dehydrogenation of n-butane. J Energ Chem, 2016, 25: 349–353

161 Cai J, Zang L, Zhao L, *et al.* Dehydrogenation characteristics of LiAlH₄ improved by *in-situ* formed catalysts. J Energ Chem, 2016, 25: 868–873

162 Diao J, Feng Z, Huang R, *et al.* Selective and stable ethylbenzene dehydrogenation to styrene over nanodiamonds under oxygen-lean conditions. ChemSusChem, 2016, 9: 662–666

163 Zhang Y, Wang J, Rong J, *et al.* A facile and efficient method to fabricate highly selective nanocarbon catalysts for oxidative dehydrogenation. ChemSusChem, 2017, 10: 353–358

164 Diao J, Zhang Y, Zhang J, *et al.* Fabrication of MgO–rGO hybrid catalysts with a sandwich structure for enhanced ethylbenzene dehydrogenation performance. Chem Commun, 2017, 53: 11322–

11325

165 Gläsel J, Diao J, Feng Z, et al. Mesoporous and graphitic carbide-derived carbons as selective and stable catalysts for the dehydrogenation reaction. Chem Mater, 2015, 27: 5719–5725

166 Diao J, Liu H, Feng Z, et al. Highly dispersed nanodiamonds supported on few-layer graphene as robust metal-free catalysts for ethylbenzene dehydrogenation reaction. Catal Sci Technol, 2015, 5: 4950–4953

167 Sun C, Luo J, Cao M, et al. A comparative study on different regeneration processes of Pt-Sn/γ-Al$_2$O$_3$ catalysts for propane dehydrogenation. J Energy Chem

168 Peng X, Zhu J, Yao L, et al. Effect of methane co-feeding on the selectivity of ethylene produced from oxidative dehydrogenation of ethane with CO$_2$ over a Ni-La/SiO$_2$ catalyst. J Energ Chem, 2013, 22: 653–658

169 Corbet J, Mignani G. Selected patented cross-coupling reaction technologies. Chem Rev, 2006, 106: 2651–2710

170 Balanta A, Godard C, Claver C. Pd nanoparticles for C–C coupling reactions. Chem Soc Rev, 2011, 40: 4973–4985

171 Johansson Seechurn C, Kitching M, Colacot T, et al. Palladium-catalyzed cross-coupling: a historical contextual perspective to the 2010 Nobel Prize. Angew Chem Int Ed, 2012, 51: 5062–5085

172 Valente C, Calimsiz S, Hoi K, et al. The development of bulky palladium NHC complexes for the most-challenging cross-coupling reactions. Angew Chem Int Ed, 2012, 51: 3314–3332

173 Li H, Johansson Seechurn C, Colacot T. Development of pre-formed Pd catalysts for cross-coupling reactions, beyond the 2010 Nobel Prize. ACS Catal, 2012, 2: 1147–1164

174 Lamblin M, Nassar-Hardy L, Hierso J, et al. Recyclable heterogeneous palladium catalysts in pure water: sustainable developments in Suzuki, Heck, Sonogashira and Tsuji-Trost reactions. Adv Synth Catal, 2010, 352: 33–79

175 Yin L, Liebscher J. Carbon−carbon coupling reactions catalyzed by heterogeneous palladium catalysts. Chem Rev, 2007, 107: 133–173

176 Choi H, Woo H, Jang S, et al. Ordered mesoporous carbon supported colloidal Pd nanoparticle based model catalysts for Suzuki coupling reactions: impact of organic capping agents. ChemCatChem, 2012, 4: 1587–1594

177 Köhler K, Heidenreich R , Soomro S , et al. Supported palladium catalysts for suzuki reactions: structure-property relationships, optimized reaction protocol and control of palladium leaching. Adv Synth Catal, 2008, 350: 2930–2936

178 Li Y, Fan X, Qi J, et al. Palladium nanoparticle-graphene hybrids as active catalysts for the Suzuki reaction. Nano Res, 2010, 3: 429–437

179 Moussa S, Siamaki A, Gupton B, et al. Pd-partially reduced graphene oxide catalysts (Pd/PRGO): laser synthesis of Pd nanoparticles supported on PRGO nanosheets for carbon–carbon cross coupling reactions. ACS Catal, 2012, 2: 145–154

180 Metin Ö, Ho S, Alp C, et al. Ni/Pd core/shell nanoparticles supported on graphene as a highly active and reusable catalyst for Suzuki-Miyaura cross-coupling reaction. Nano Res, 2013, 6: 10–18

181 Li Y, Barløse C, Jørgensen J, et al. Cover picture: asymmetric catalytic aza-diels-alder/ring-closing cascade reaction forming bicyclic azaheterocycles by trienamine catalysis. Chem Eur J,

2017, 23: 38–41

182 Quinn T, Choudhury P. Direct oxidation of methane to methanol on single-site copper-oxo species of copper porphyrin functionalized graphene: a DFT study. Mol Catal, 2017, 431: 9–14

183 Impeng S, Khongpracha P, Sirijaraensre J, et al. Methane activation on Fe- and FeO-embedded graphene and boron nitride sheet: role of atomic defects in catalytic activities. RSC Adv, 2015, 5: 97918–97927

184 Sirijaraensre J, Limtrakul J. Modification of the catalytic properties of the Au$_4$ nanocluster for the conversion of methane-to-methanol: synergistic effects of metallic adatoms and a defective graphene support. Phys Chem Chem Phys, 2015, 17: 9706–9715

185 Impeng S, Khongpracha P, Warakulwit C, et al. Direct oxidation of methane to methanol on Fe–O modified graphene. RSC Adv, 2014, 4: 12572–12578

186 Russell J, Zapol P, Král P, et al. Methane bond activation by Pt and Pd subnanometer clusters supported on graphene and carbon nanotubes. Chem Phys Lett, 2012, 536: 9–13

187 Bian J, Wei X, Wang L, et al. Graphene nanosheet as support of catalytically active metal particles in DMC synthesis. Chin Chem Lett, 2011, 22: 57–60

188 Kumar S, Kumar P, Jain S. Graphene oxide immobilized copper phthalocyanine tetrasulphonamide: the first heterogenized homogeneous catalyst for dimethylcarbonate synthesis from CO$_2$ and methanol. J Mater Chem A, 2014, 2: 18861–18866

189 Bian J, Xiao M, Wang S, et al. Highly effective synthesis of dimethyl carbonate from methanol and carbon dioxide using a novel copper–nickel/graphite bimetallic nanocomposite catalyst. Chem Eng J, 2009, 147: 287–296

190 Kumar S, Khatri O, Cordier S, et al. Graphene oxide supported molybdenum cluster: first heterogenized homogeneous catalyst for the synthesis of dimethylcarbonate from CO$_2$ and methanol. Chem Eur J, 2015, 21: 3488–3494

191 Ren Y, Fan G, Wang C. Aqueous hydrodechlorination of 4-chlorophenol over an Rh/reduced graphene oxide synthesized by a facile one-pot solvothermal process under mild conditions. J Hazard Mater, 2014, 274: 32–40

192 Zhao F, Kang L. The neglected significant role for graphene-based acetylene hydrochlorination catalysts–intrinsic graphene defects. ChemistrySelect, 2017, 2: 6016–6022

193 Zhao F, Wang Y, Kang L. A density functional theory study on the performance of graphene and N-doped graphene supported Au$_3$ cluster catalyst for acetylene hydrochlorination. Can J Chem, 2016, 94: 842–847

Author contributions   Liu H concieved the work. Huang F wrote the paper. All authors contributed to the general discussion.

Conflict of interest   The authors declare that they have no conflict of interest.

Fei Huang received his MSc degree in industrial catalysis from Southwest Petroleum University in 2016. Now he is a PhD candidate in Prof. Hongyang Liu & Dangsheng Su's group at Catalysis and Materials Division of Shenyang National Laboratory for Materials Science, the Institute of Metal Reaserch, Chinese Academy of Sciences. His current research is nanocarbon supported metal catalysis and application in hydrogenation reaction.

Hongyang Liu received his PhD degree from Dalian Institute of Chemical Physics, Chinese Academy of Sciences in 2009. He then worked as a postdoctoral fellow at the University of Missouri, US (2009–2011). Currently, He is an associate professor at the Institute of Metal Research, Chinese Academy of Sciences. His research interest is nanocarbon based catalysts for heterogeneous catalytic reactions.

石墨化纳米碳材料负载金属催化剂: 合成、性质及其在多相催化中的应用

黄飞[1,2], 刘洪阳[1*], 苏党生[1]

摘要 石墨化纳米碳材料可作为一种理想的非均相催化剂载体. 它们独特的物理化学性质, 包括高比表面积, 高吸附能力, 优良的热稳定性和机械稳定性, 优异的电子特性和可调变的孔径结构, 这些性质使其能够锚定和分散活性金属. 因此, 石墨化纳米碳作为一种载体材料被广泛用于催化过程. 本综述总结了近年来石墨化纳米碳作为负载型催化剂载体在氧化、 加氢、 脱氢、 碳-碳偶联等气-固相或液-固相反应体系中的相关应用. 重点介绍了石墨化纳米碳负载金属催化剂形态特性和表征, 以及相较于其他相关催化剂表现出的不同的催化性能. 并对这一领域存在的挑战和机遇作了简要讨论.